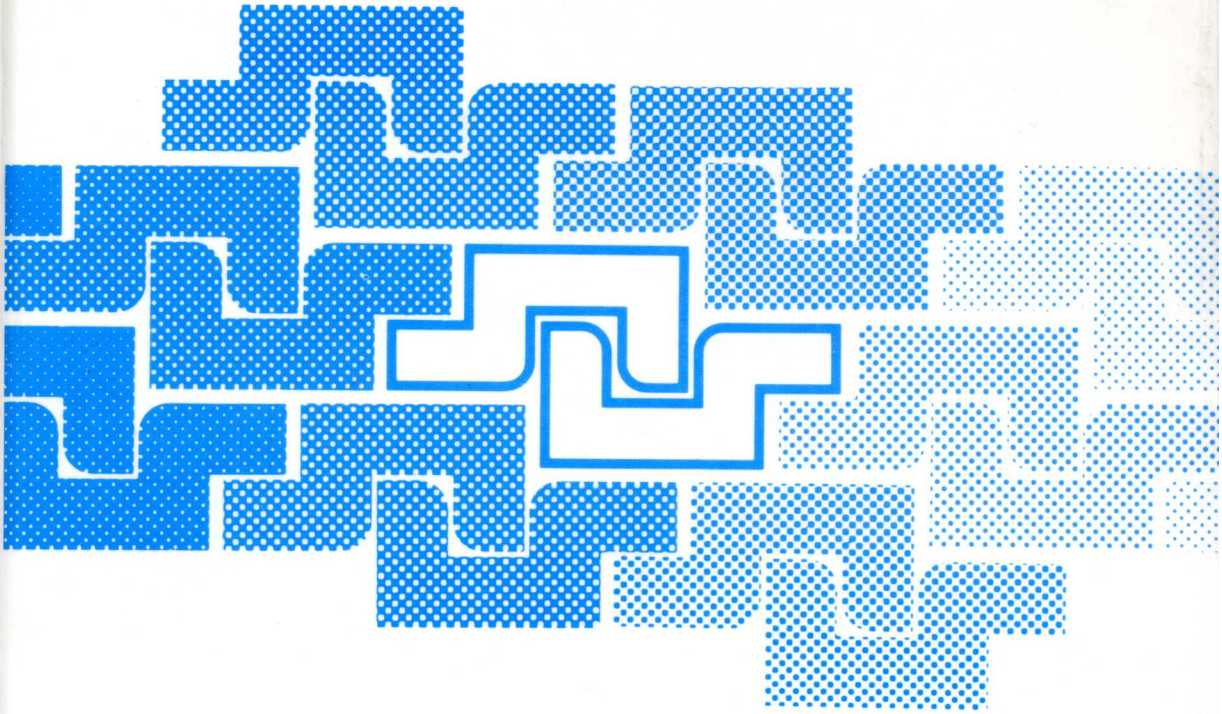

Chaos, Order, and Patterns

Edited by

Roberto Artuso

Predrag Cvitanović and

Giulio Casati

NATO ASI Series

Series B: Physics Vol. 280

Proceedings of a NATO Advanced Study Institute
on Chaos, Order, and Patterns,
held June 25-July 6, 1990,
in Lake Como, Italy

Library of Congress Cataloging in Publication Data

NATO Advanced Study Institute on Chaos, Order, and Patterns (1990: Centro di cultura scientifica "A. Volta")
Chaos, order, and patterns / edited by Roberto Artuso, Predrag Cvitanović, and Giulio Casati.
p. cm.—(NATO ASI series. Series B: Physics; vol. 280)
"Proceedings of a NATO Advanced Study Institute on Chaos, Order, and Patterns, held June 25-July 6, 1990, in Lake Como, Italy"—T.p. verso.
Includes bibliographical references and index.
ISBN 0-306-44080-6
1. Chaotic behavior in systems—Congresses. 2. Pattern perception—Congresses. I. Artuso, Roberto. II. Cvitanović, Predrag. III. Casati, Giulio, 1942- . IV. North Atlantic Treaty Organization. Scientific Affairs Division. V. Title. VI. Series: NATO ASI Series. Series B, Physics; v. 280.
Q172.5.C45N377 1990 91-42273
003'.7—dc20 CIP

ISBN 0-306-44080-6

A Division of Plenum Publishing Corporation
233 Spring Street, New York, N.Y. 10013

Printed in the United States of America

CONTENTS

PATTERNS IN CHAOS

Boris V. Chirikov
notes prepared with assistance of Svend E. Rugh

Institute of Nuclear Physics, 630090 Novosibirsk, U.S.S.R.

Classification of chaotic patterns in classical Hamiltonian systems is given as a series of levels with increasing disorder. Overview of critical phenomena in Hamiltonian dynamics is presented, including the renormalization chaos, based upon the fairly simple resonant theory. First estimates for the critical structure and related statistical anomalies in arbitrary dimensions are discussed.

Introduction

The main idea I would like to convey here is the inexhaustible diversity and richness of the dynamical chaos whatever description you choose: trajectories, statistics or, recently, renormalization. The importance of this relatively new phenomenon - the dynamical chaos - is in that it presents, even in very simple models to be discussed below, the surprising complexity of the structures and evolution characteristic of a broad range of processes in nature, including the highest levels of its organization. Moreover, dynamical chaos is the only stationary source of any new information and, hence, a necessary part of creative activity, science included. This is a direct consequence of the Alekseev-Brudno theorem and Kolmogorov's development of the information theory (see e.g. refs. [1,2]). The chaos is not always that bad!

Below I restrict myself to the classical mechanics only. The so-called "quantum chaos" is another story (see e.g. refs. [3,4]). Let me just mention that apart from very exotic examples, there is no "true" chaos in quantum mechanics, contrary to common belief. On the other hand, the unavoidable statistical element of quantum mechanics related to the measurement is very likely associated with the classical chaos in a measuring apparatus.

With a bit of imagination and fantasy one may even conjecture that any macroscopic event in this World, which formally is the result of some quantum "measurement", would be impossible without chaos.

Also, I am not going to consider any dissipative models (very important in practical applications) because they are not as fundamental as Hamiltonian systems. Besides,

Chaos, Order, and Patterns, Edited by R. Artuso *et al.*
Plenum Press, New York, 1991

strictly speaking, the dissipative systems are not purely dynamical as the dissipation is inevitably related to some noise.

In what follows I take a physicist's approach to the problem: my presentation will be based on a simple (sometimes even qualitative) theory, combined with the results of extensive numerical (computer) experiments. For a good physical overview of dynamics and chaos see books [5,6].

The principal concept of such a theory is the nonlinear resonance whose phase space picture (quite familiar by now) is depicted in Fig. 4 below. An essential part of this resonance structure is a pair of periodic orbits, the most important being the unstable one as it gives rise to the separatrix and, under almost any perturbation, to the surrounding chaotic layer around. This is precisely the place where chaos dawns.

Again, I have to restrict myself to a simpler case of strong nonlinearity which does not vanish with perturbation. A very interesting weakly nonlinear resonance will be briefly mentioned in section 1.2. below.

These lectures are organized as follows. In section 1 simple models, currently extensively used in the studies of nonlinear phenomena and chaos, are described. They will represent the whole spectrum of complexity classified in section 2. The main sections 3 and 4 are devoted to a detailed description of the so-called critical phenomena in dynamics which reveal the most complicated behavior presently known.

1 Simple models

First, let us consider a number of simple models currently very popular in the studies of dynamical chaos. Most of them are specified by some mappings, or maps, rather than by differential equations. This considerably simplifies both the theoretical analysis and, especially, the computer experiments. In conservative Hamiltonian systems the chaos requires two degrees of freedom, at least. The corresponding Poincaré map is two-dimensional.

1. Strong nonlinearity [7]. Below we shall consider 2D maps of the following form:

$$\overline{y} = y + f(x) \quad ; \quad \overline{x} = x + g(\overline{y}) \tag{1.1}$$

This map is area-preserving, or canonical, reflecting the Hamiltonian nature of the model. The function $f(x)$, periodic in x, describes a perturbation, usually assumed to be small. Hence, y is the unperturbed motion integral. The function $g(y)$, even if it is linear (see eq. (1.6) below), represents the nonlinearity of the x oscillation.

The simplest example of an analytic perturbation is given by

$$f(x) = K \sin x \tag{1.2}$$

We shall also consider a smooth perturbation specified by the Fourier series

$$f(x) = \sum_m f_m e^{imx} \quad ; \quad f_m \sim K |m|^{-\beta} \tag{1.3}$$

where β is the smoothness parameter. The term 'smooth' actually means sufficiently smooth. For $\beta = 2$, for example, the function $f(x)$ is continuous but the first derivative is discontinuous.

I mention two particular forms of nonlinearity. The first one

$$g(y) = \lambda \ln|y| \tag{1.4a}$$

models the motion near the separatrix of a nonlinear resonance, so that the map (1.1) with its nonlinearity and perturbation (1.2) describes, in particular, a separatrix chaotic layer [7].

Another form of nonlinearity

$$g(E) = 2\pi\omega(-2\,E)^{-3/2} \tag{1.4b}$$

corresponds to the Coulomb interaction, or the Kepler law. Here it is convenient to use the unperturbed energy $E < 0$ as a dynamical variable, and ω is the perturbation frequency (see ref. [4]).

The map (1.1) with the nonlinearity (1.4 b) and perturbation (1.2) is called the Kepler map, and it is applied in both celestial mechanics and atomic physics. In the former case the motion of comet Halley driven by Jupiter and Saturn was proved to be chaotic [8]. In atomic physics the Kepler map is a simple model to describe, in particular, a new type of photoelectric effect, the so-called diffusive ionization of Rydberg (highly excited) atoms [9].

The two latter examples show that the map (1.1) can be considered also as a model for time-dependent dynamical systems driven by a periodic perturbation. This is, of course, simply a very convenient approximation in which the feedback from the perturbed degree of freedom to the perturbing one is completely neglected. Then, the model (1.1) can be described by the Hamiltonian

$$H(x,y,t) = G(y) + F(x)\delta_1(t) \;\rightarrow\; G(y) + K\sum_m \cos(x - 2\pi m t) \tag{1.5}$$

where $\delta_1(t)$ is a δ -function of period 1 (one map's iteration), $G'(y) = g(y)$, $F'(x) = -f(x)$, and the last series represents the perturbation (1.2).

The fairly simple map (1.1) can be simplified still further by linearizing the second equation. In this way we arrive, upon appropriate change of the action y , at the so-called standard map

$$\overline{y} = y + K\,\sin x \;\;;\;\; \overline{x} = x + \overline{y} \tag{1.6}$$

which describes the original model (1.1) locally in y , and which is also very popular now in studies of nonlinear phenomena in Hamiltonian systems. The model (1.6) is completely characterized by a single parameter K. In the Hamiltonian representation (1.5) the 'kinetic energy' for the standard map is $G(y) = y^2/2$. Since x is an angle (phase) variable and y is the angular momentum, the model (1.6) is also called the 'kicked rotator'.

Each term in the series (1.5) describes a particular first order (primary) nonlinear resonance with the 'pendulum' Hamiltonian (for the standard map)

$$H_m = \frac{y^2}{2} + K\,\cos(x - 2\pi m t) \tag{1.7}$$

The resonant value of momentum $y_m = \dot{x}_m = 2\pi m$. In variables $\tilde{x} = x - 2\pi m t$ and $\tilde{y} = y - y_m$ any single resonance is a conservative system. Its motion is strictly bounded in y by the resonance width $\Delta y_m = 4\sqrt{K}$, due to the nonlinearity, i.e., the dependence of the frequency $\dot{x} = y$ on the momentum y .

2. Weak nonlinearity [10]. The structure of the resonance drastically changes if we add to the Hamiltonian (1.7) the term $\omega_0^2 x^2/2$:

$$H_m = \frac{y^2}{2} + \frac{\omega_0^2 x^2}{2} + K\ \cos(x - 2\pi m t) \tag{1.8}$$

which breaks down the integrability of the system for any $\omega_0 \neq 0$.

Actually, the model (1.8) is quite different from the model (1.7), as now the variable x is no longer confined to the interval $(0, 2\pi)$, and y is not the angular momentum. One may interpret the Hamiltonian (1.8) as describing a particle-wave interaction. Such models have been studied by many authors in plasma physics (see, e.g., ref. [5]), yet the true understanding has been achieved only recently (see, e.g., ref. [10]). The peculiarity of the model (1.8) is the weak nonlinearity, i.e., the unperturbed ($K = 0$) oscillation is linear (isochronous), which turns out to be a much more difficult problem as compared with strong (unperturbed) nonlinearity (1.4). The resonance is now determined not by initial conditions but by the parameters of the model: $2\pi m = n\ \omega_0$ with any integer $n \neq 0$. In the action-angle variables (I, ϕ) of the harmonic oscillator a single resonance is approximately described by the Hamiltonian

$$H_m \approx K\ J_m(a)\ \cos(m\phi + \frac{\pi m}{2}) \tag{1.9}$$

where $a = (2\ I/\omega_0)^{1/2}$ is the oscillation amplitude, and J_m the Bessel function. There are now infinitely many stable and unstable periodic orbits (instead of two for strong nonlinearity) while the separatrices, connecting unstable points, form an unbounded network on the phase plane (I, ϕ). As a result, even a single weakly nonlinear resonance can make the motion completely unstable and unbounded.

2 Levels of Disorder

In this section I shall attempt to 'organize' the great variety of chaos into a series of levels of increasing disorder and complexity.

0. Complete integrability [15] This, zero-th level of the maximal order is characterized by a stable and dynamically predictable motion in terms of individual trajectories. The motion is quasiperiodic, i.e., of a purely discrete spectrum. One may call this a simple dynamics. Yet, in the general theory of dynamical systems this 'simple' motion includes the whole quantum chaos, typically on a finite time scale (see, e.g., ref. [3]). The latter is dynamically equivalent to a many-dimensional linear oscillator which is apparently the simplest model of the quantum chaos [11]. On the other hand, in the formal thermodynamic limit of infinitely many degrees of freedom, this model has provided the foundations of the traditional statistical mechanics, both classical and quantal, for macroscopic systems (for a rigorous theory see, e.g., ref. [12]).

The standard map, as the simplest model, is completely integrable for $K = 0$ only, that is in the unperturbed limit. In this case $y = const$ is the motion integral, and $x = 2\pi r t$ where the quantity

$$r = \frac{\omega}{2\pi} = \frac{\Delta x}{2\pi\ \Delta t} \tag{2.1}$$

is called the rotation number. This very important parameter of a trajectory is the ratio

of motion frequency (ω) to that of the perturbation frequency (2π). Particularly, this ratio determines resonances (with zero perturbation in this limit !) which correspond to rational $r = p/q$. Any resonant trajectory is just q separate points on the phase plane (x, y) . For irrational r the trajectory is a continuous straight line $y = 2\pi r$, called the invariant curve.

In spite of great successes in constructing the whole families of completely integrable systems (see, e.g., ref. [13]), they are all exceptional, or non-generic, in the sense that almost any perturbation destroys the integrability.

1. KAM integrability [14] is the generic property of a completely integrable system under sufficiently weak perturbation. The theory of such systems had been initiated by Kolmogorov and was essentially developed by Arnold and Moser (see, e.g., ref. [15]), hence, the abbreviation KAM.

For the standard map this first level of disorder corresponds to a non-zero $K \to 0$. Most invariant (KAM) curves survive weak perturbation, i.e., they are only slightly deformed but remain continuous and, hence, unpenetrable for other trajectories. For this reason the KAM curve is called an absolute barrier (for the motion). This property depends on the rotation number r of the curve which must be sufficiently irrational for the stability against perturbation. Hence, the importance of the parameter r which is used as the label for identification of a given KAM curve at different perturbations.

Curves with resonant $r = p/q$ are all destroyed by any perturbation to form a different structure of the nonlinear resonance (Fig.4). However, the nonintegrable part of this structure is confined to an exponentially narrow chaotic layer only. From a physical point of view such motion can in most cases be considered integrable to a very high accuracy. This is reminiscent of the adiabatic invariance, very important in physics even though it is not exact. Actually, there is a deep relation between the two, and we call KAM integrability the inverse adiabaticity [14,16].

Approximately, the dynamics on this level is as simple as the previous one. Yet, the chaotic component of motion, being of an exponentially small measure, is everywhere dense. As a result, the whole motion structure becomes very complicated. For more than two degrees of freedom the phase space is cut through by a connected network of channels which support global diffusion [7]. Even though the rate of this Arnold diffusion is also exponentially small, it may be important in some special cases. For a weakly nonlinear system the Arnold diffusion is possible even in two degrees of freedom as well (see for instance [10]) in the model (1.8).

2. Complete chaos [20]. Now we turn to the opposite limiting case, the case of fully chaotic motion. In the standard map, as $K \to \infty$, there is a single chaotic component of motion stretched over the whole phase space (cylinder) of the model. The motion spectrum is purely continuous, while a typical individual trajectory is most complicated. The latter means that Kolmogorov's complexity, which is equal to the information associated with the trajectory per unit time, is finite, and equal to the rate of local instability of the motion [1]. Hence, the dynamics on this level is so complicated that the trajectory actually loses its physical meaning.

Nevertheless, the dynamical equations, e.g., map (1.6), can still be applied to describe completely the statistical properties of the unstable motion. Moreover, on this level the statistics turns out to be very simple and already well known from the tradi-

tional statistical mechanics. For example, in the standard map it is simply a homogeneous diffusion in y with the rate

$$D_y \equiv \frac{<(\Delta y)^2>}{t} = \frac{K^2}{2} C(K) \to \frac{K^2}{2} \tag{2.2}$$

where the function $C(K)$ accounts for the dynamical correlation of the phase X, and $C(K) \to 1$ as $K \to \infty$ [17]. For this reason the complexity of the motion on this level is still not the highest one.

3. Critical phenomena: Scale invariance [21]. For a typical (generic) perturbation, neither very weak nor very strong, the whole structure of motion is most complicated because the phase space is generally divided in many separate domains with both regular and chaotic motions. In the standard map, for example, such an intricate behavior

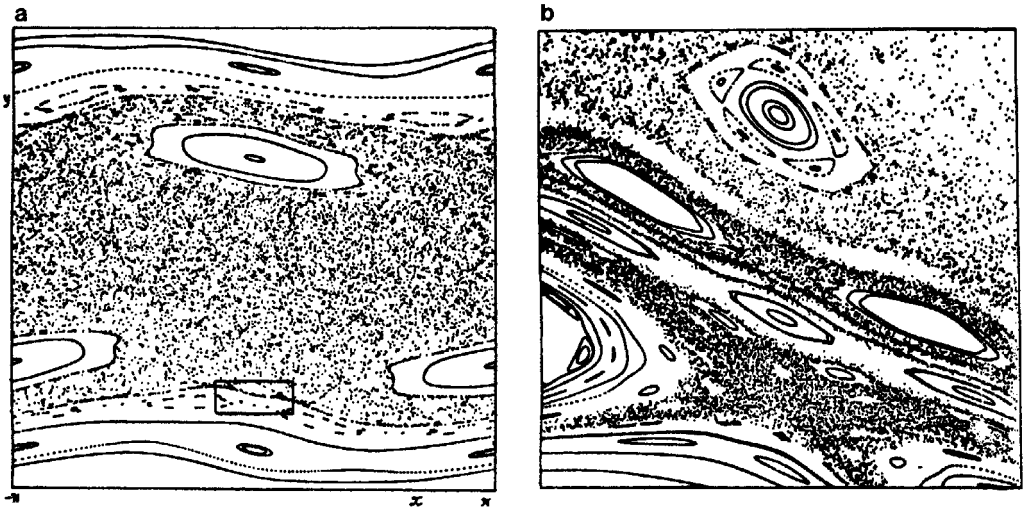

Figure 1. An example of critical structure in the map (3.1) with $\lambda = 5$; Scattered points belong to a single chaotic trajectory: (a) the whole chaotic layer; (b) enlarged part near the chaos border $y \approx -\lambda$ where the motion is described locally by the standard map (1.6) with $K \approx 1$ [19].

corresponds to $K \sim 1$ (see Fig.1), i.e., around the global critical perturbation $K = K_G \approx 1$. The latter is the border between strictly bounded motion for any initial conditions ($K \leq K_G$) and unbounded motion for some initial conditions ($K > K_G$).

In the unbounded chaotic component (for $K > K_G$) the motion is still diffusive with the rate [18]

$$D_y \approx 0.3\,(K - K_G)^3 \tag{2.3}$$

vanishing towards the critical perturbation (cf. eq. (2.2) where the correlation $C(K) \approx 0.6\,(K - K_G)^3/K^2$). The main difficulty here is a hierarchical (fractal) structure of the chaotic component. The invariance of the phase space, does not help in this case. The ultimate origin of this complexity is the phase space border between the chaotic and the

regular components of motion, which also leads to very peculiar statistical properties of the chaotic motion (see section 4).

The chaos border makes both the individual (chaotic) trajectories as well as the statistical properties of the motion very complicated. Is there any way to simplify the description of such a motion? Or: is it possible to find any order in this mess? Surprisingly it is possible indeed, in some cases, if one compares the critical structure at different scales in the phase plane (section 3.3). Asymptotically, as you enlarge the structure more and more, it repeats itself exactly, with all the dynamical and statistical complexity (see also Fig.5 below)! This peculiar property is called the scale invariance, and it is described by the so-called renormalization group or in brief, renormgroup.

4. Critical phenomena: Renormalization chaos [22]. The variation of the motion structure with the scale in phase space can be considered as a certain abstract dynamics (see section 3.4) which we termed the renormalization dynamics, or renormdynamics [22]. Here the scale plays a role of 'time' and we call it renormalization time. The simplest case of any dynamics is a fixed point (for maps) which in renormalization dynamics corresponds to the scale invariance described above (see also section 3.3). But typically the dynamics is chaotic, and so there must be a sort of renormalization chaos (renormchaos) as well. Guided by this analogy, we have indeed found such chaos [22]!

In this case the renormalization is as complicated as an individual chaotic trajectory of the original dynamical system. Yet, some remnants of order still persist, namely, the universality of renormalization. This means that asymptotically, for a big renormalization time, i.e., for small spatial scales, the critical structure is a universal functional of a single irrational number - the rotation number r_c of the critical curve, e.g., the border curve, in almost any 2D map [21].

Moreover, one can introduce the renormalization statistics ,i.e., statistical description of the renormalization. Then, for almost any r_c, the renormalization statistics is the same, i.e. universal, and it is fairly simple.

5. Critical phenomena: The breakdown of universality [23]. Recently, the first example of still more complicated behavior has been found in ref. [23], where a quasiperiodic driving perturbation was studied. Specifically, the standard map (1.6) was used in numerical experiments with periodically time-dependent parameter $K(t) = K_1 + K_2 \cos(2\pi r_2 t)$, incommensurable with the time step of the map.

To some extent such a model also represents a higher-dimensional behavior. A critical curve is now characterized by the two irrational rotation numbers r_1 , r_2 . For a particular choice of irrationals r_1 , r_2 it was found that the renormalization dynamics depends on the parameters K_1 and K_2. It is thus not clear whether such breakdown is typical. If so, one would expect also a more complicated renormalization statistics.

Here we have come to the frontier of the unknown. Currently, there is no idea what would imply still higher levels of disorder, if such existed.

3 Critical Dynamics

In this section I consider in some detail the two levels of disorder briefly described in section 2 above (levels 3 and 4). This work was done in collaboration with D.L.Shepelyansky.

1. Statistical 'anomalies' in dynamical chaos [24]. We encountered the critical phenomena in studying some statistical properties of motion in a simple map

$$\overline{y} = y + \sin x \quad ; \quad \overline{x} = x + \lambda \ln |\overline{y}| \tag{3.1}$$

of the type described in section 1.1 above. Our studies were stimulated by ref. [25], with the intriguing title 'Numerical Experiments in Stochasticity and Heteroclinic Oscillation'. Actually, the motion in a chaotic separatrix layer had been studied, and we went on with a much simpler model (3.1) (see ref. [7]).

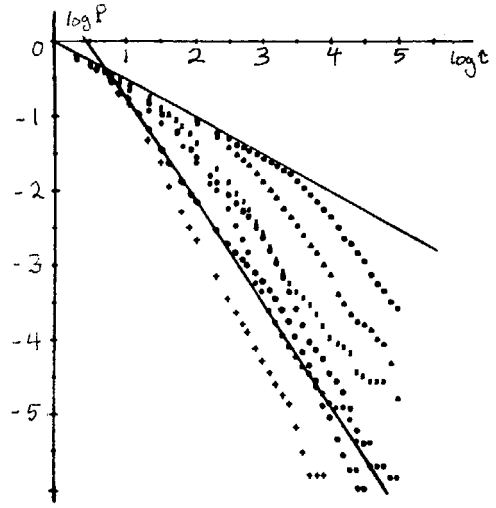

Figure 2. Poincaré recurrences in the chaotic layer of map (3.1) for various $\lambda = 1$ (lower points) through 100 (upper points). The two straight lines are power laws with exponents -0.5 and -1.37, respectively (after ref. [24]).

We studied the statistics of the times t_n when a trajectory crosses the symmetry line $y = 0$. We call the differences $\tau_n = t_{n+1} - t_n$ the Poincaré recurrence times. The same was implicitly done in ref. [25]. Our results are shown in Fig. 2, where $P(\tau)$ is the (integral) probability for $\tau_n > \tau$. The initial part of the distribution is very close to

$$P_f = \frac{1}{\sqrt{\tau}} \quad ; \quad \tau \geq 1 \ , \tag{3.2}$$

and is explained by a free homogeneous diffusion within the chaotic layer before the trajectory reaches the layer border ($y_b \approx \lambda$). This takes the time

$$\tau_f \approx 0.3 \ \lambda^2 \ , \tag{3.3}$$

where the coefficient was estimated from the numerical data.

Curiously, in ref. [25] only this (trivial) part of the distribution $P(\tau)$ was observed. It was the cost for the authors' great concern about the exponential error growth at a

chaotic trajectory. To overcome the instability, the computation was performed with the record accuracy of 358 decimal places! As a result, the chaotic trajectory can be followed during a rather short time interval.

Error growth is a serious problem, indeed, as the structural stability of Hamiltonian motion is almost unknown rigorously. Yet, all the numerical experience up to now strongly suggests such stability and, hence, the stability of statistical properties which are of primary interest for chaotic motion. Besides, only structural stability justifies the use of various simple models and approximations.

In our studies of the model (3.1) we checked directly that the distribution $P(\tau)$, which is a statistical property of the motion, does not depend on a particular trajectory within expected statistical fluctuations. The latter noticeably influence the lowest part of the distribution $P(\tau)$ where the number of events per histogram bin is ~ 1 (see Fig.2).

The most interesting is the asymptotics of $P(\tau)$ for $\tau \gg \tau_f$ (3.3). This part characterizes the motion structure of the chaos border at $|y| = y_b \approx \lambda$, or, as we call it, the critical structure.

The following features of the $P(\tau)$ asymptotics seem to be of importance. First, the distribution is a power law and not an exponential:

$$P(\tau) \approx \frac{\tau_f^{p-1/2}}{\tau^p} \; ; \; \tau \geq \tau_f \; ; \; <p> \approx 1.5 < 2 \tag{3.4}$$

This suggests a hierarchical (fractal) structure of the border. The accuracy of the numerical value for p is not very good, yet we are sure that the important inequality (3.4) always holds.

On the other hand, the distribution $P(\tau)$ behaves as a power law only approximately, in the sense of an average. Irregular oscillations of the local exponent $p(\tau) \equiv d\ln P/d\ln\tau$ clearly show up in Fig.2. These do not depend on the trajectory and, hence, are not statistical fluctuations but characterize the structure of the chaos border. Such structure with a variable exponent $p(\tau)$ is now called multifractality (see,e.g., ref. [26]).

The statistics of the Poincaré recurrences $P(\tau)$ proved to be the most convenient and reliable numerical data to study (cf. ref. [25]). On the other hand, this statistics is directly related to the most important statistical property of time correlation functions [27], such as

$$C_y(\tau) = \frac{\overline{y(t)\,y(t+\tau)}}{\overline{y^2(t)}} \tag{3.5}$$

which characterizes the 'sticking' of the trajectory near the border. Notice that $\overline{y(t)} = 0$ for the map (3.1).

Indeed, the correlation is proportional to the sticking time, that is (cf. ref. [27])

$$C_y \sim \frac{\tau\, P(\tau)}{<\tau>} \sim \tau^{-p_c} \; ; \; p_c = p - 1 < 1 \tag{3.6}$$

for $\tau \geq \tau_f$. Here $<\tau> \approx 3\lambda$ is the mean recurrence time, and the latter important inequality follows from eq. (3.4) (see also Fig.3b). For chaotic motion $C_y \to 0$ as $\tau \to \infty$ (mixing property), hence $p_c > 0$, and, for bounded motion, $p > 1$. Notice, also, that due to the ergodicity of the motion $C_y \sim \mu(\tau)$, the measure of the sticking domain (a strip) $\sim |y - y_b|/y_b$, where $y_b \approx \lambda$, is the half-width of the chaotic layer for the map (3.1).

Slow correlation decay due to the sticking of a chaotic trajectory near the chaos border, and especially the inequality (3.6) is responsible for all other statistical 'anomalies' of the motion with a chaos border to be discussed below. A power law decay (3.6) is especially remarkable in view of the strong exponential instability of the motion which is characterized by a positive Lyapunov exponent Λ_+ and the KS-entropy (per map's iteration): $h = \Lambda_+ \approx 0.7$ (see section 6.3 in ref. [7]). The apparent contradiction is explained as follows. The instability rate h is mainly determined by the central part of the chaotic layer while the sticking is a peripheral effect which has a negligible impact

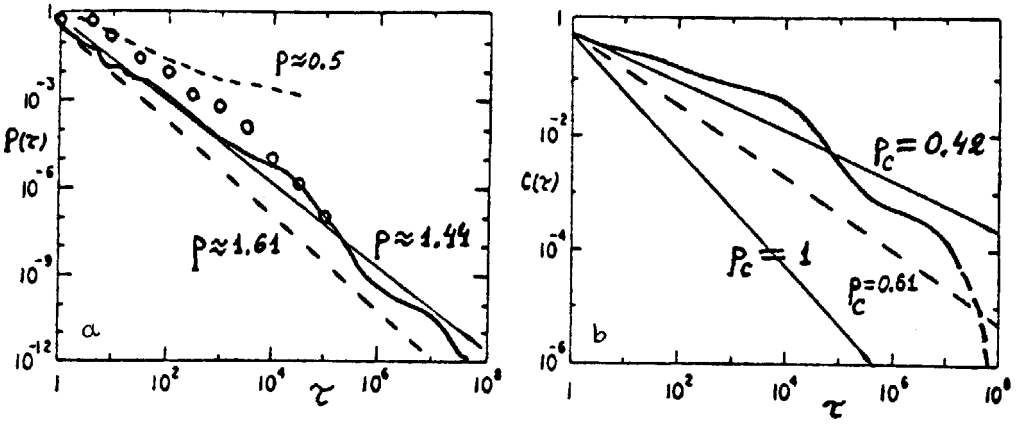

Figure 3. Statistical properties of motion with chaos border: (a) Poincaré recurrences; (b) correlation decay. Solid curves are for the map (3.7) [27] while circles are our data for $\lambda = 3$. Straight lines indicate power laws with the exponents shown. The dashed curve is the effect of noise [22].

on the mean local instability. In other words, the KS-entropy does not discern such statistical anomalies. This can be accomplished using the Renyi entropy K_q which is a generalization of $h = K_1$ (see, e.g., ref. [28]), and which drops to zero for all values of the parameter $q > 1$ in the presence of a chaos border [29].

The critical phenomena at the chaos border and the related statistical anomalies are 'universal' (a very popular word in this field of research!) in that they are approximately the same in any 2D map. In Fig.3(a), for example, our results are compared with those in ref. [27] for a different map on the torus

$$\overline{y} = y + 2(x^2 - a^2) \;\; ; \;\; \overline{x} = x + \overline{y} \;\; , \tag{3.7}$$

with a closed chaos border surrounding the domain of regular motion around the stable fixed point at $y = 0$; $x = -a$ $(0 < a < 1)$. Notice that the two distributions $P(\tau)$ are not identical but rather similar (see below).

2. The resonant theory [30]. To understand the statistical anomalies described above we have developed a resonant theory of critical phenomena in dynamics [30,31]. Let us begin with the simpler problem of an isolated critical KAM curve whose rotation number is some irrational r. According to the KAM theory most invariant curves

are preserved under a sufficiently weak perturbation in the sense that they remain continuous and are only slightly deformed by the perturbation. The theory of critical phenomena follows the transformation of a KAM curve all the way up to the critical perturbation which destroys the curve.

The critical perturbation, e.g. $K_c(r)$ for the standard map, crucially depends on the arithmetic nature of r. Remember that for the everywhere dense set of rationals $r = p/q$, the critical $K_c(p/q) = 0$ (section 2.1). The whole dependence $K_c(r)$ is a fractal function [32].

The physical explanation of this behavior lies in the nature of resonances. Their profound impact on the critical structure is clearly seen in all numerical data (see,

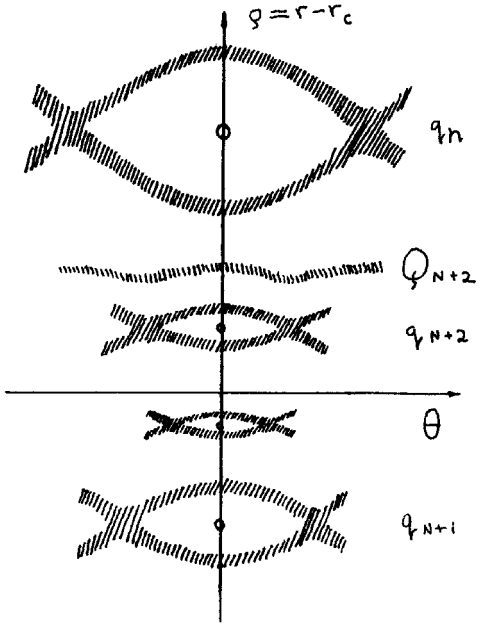

Figure 4. Outline of the critical structure with a few principal resonances, represented by the separatrix chaotic layers (hatched) and stable periodic orbits (circles), and the corresponding scales q_n. Another chaotic layer Q_n is a bottleneck between the scales (section 4.3).

e.g., Fig.1). For irrational r the principal resonances correspond to the best rational approximations of r, i.e., the convergents $r_n = p_n/q_n$ of the infinite continued fraction

$$r = \frac{1}{m_1 + \frac{1}{m_2 + \ldots}} \equiv [m_1, m_2, \ldots] \; ; \tag{3.8}$$

$$r_n = [m_1, \ldots\ldots, m_n] \to r \;\; , \;\; n \to \infty$$

The arithmetic of continued fractions gives for almost any r

$$|\rho_n| \equiv |r_n - r| \sim \frac{1}{q_n^2} \sim |r_{n+1} - r_n| \tag{3.9}$$

From a physical viewpoint, ρ_n is the detuning of the n-th principal resonance with respect to the critical motion. Then, from the resonance overlap criterion [7], the main critical scaling, or the criticality condition, is

$$\Delta \rho_n \sim |\rho_n| \sim \frac{1}{q_n^2} \tag{3.10}$$

where $\Delta\rho_n$ is the resonance width. These resonances determine the principal scales of the critical structure whose scheme is outlined in Fig.4 (see also Fig.5 below).

To estimate $\Delta\rho_n$, we need the critical Hamiltonian which describes all resonances $r_{pq} = p/q$ (p, q any integers), and not only the primary ones $r_m = m$ from the original Hamiltonian of the type (1.5). Integer resonances $r_m = m$ are obtained in the first approximation $x_c(t) \approx 2\pi r_c t \equiv \xi_c$, the mean motion on the critical KAM curve.

Extrapolating the KAM theory (see, e.g., ref. [15]) the following expression can be assumed for the critical motion:

$$x_c(t) = \xi_c + \sum_q a_q \sin(q\xi_c) \tag{3.11}$$

Locally in y, in the standard-map approximation, the critical Hamiltonian H_c, which describes some vicinity of the critical KAM curve $r = r_c$, can be written as a natural generalization of the original Hamiltonian (1.5) (with $G(y) = y^2/2$) in the following form

$$H_c(\Theta, \rho, t) = \frac{\rho^2}{2} + \sum_{p,q} \frac{v_{pq}}{(2\pi)^2} \cos\, 2\pi(q\Theta - v_{pq}t) \tag{3.12}$$

Here $\rho = r - r_c$; $2\pi\Theta = x - \xi = x - 2\pi r t$ and $v_{pq} = p - qr_c$ are the driving frequencies. Resonances $\rho_{pq} = p/q - r_c$ are characterized by the perturbation amplitudes v_{pq} to be found below from the criticality condition. The factor $(2\pi)^2$ is introduced to recover the original Hamiltonian for which $v_{p1} = K$ (in variables Θ, ρ).

For principal resonances ($p = p_n$, $q = q_n$) the frequencies $\nu_n \sim q_n^{-1}$ are minimal, and they determine the time scales $t_n \sim \nu_n^{-1} \sim q_n$, the motion periods at the resonances. We introduce the scaled variables, e.g.,

$$T = \frac{t_n}{q_n} \sim 1 \tag{3.13}$$

which remain of the same order of magnitude on all scales n.

The width of a principal resonance $\Delta\rho_n \sim v_n^{1/2} \sim q_n^{-2}$ (see eq. (3.10)). Hence $v_n \sim q_n^{-4}$, and another scaled variable

$$V = v_n q_n^4 \sim 1 \ . \tag{3.14}$$

Now we can approximately solve the equation

$$\ddot{\Theta} = \dot{\rho} = -\frac{\partial H_c}{\partial \Theta} \approx -\left.\frac{\partial H_c}{\partial \Theta}\right|_{\Theta=0} \ .$$

The latter approximation means that we substitute mean motion ξ for $x_c(t)$. As our original model (3.1) is a map, time t is integer, and we can drop the term pt in the solution $\Theta(t)$ which then takes the form (3.11) with

$$a_q \approx \frac{q}{(2\pi)^3} \sum_p \frac{v_{pq}}{(p-qr)^2} \;\; ; \;\; a_n \sim v_n q_n^3 \sim q_n^{-1} \;\; .$$

Hence, the longitudinal scaled amplitude

$$A = a_n q_n \sim 1 \;\; , \tag{3.15}$$

and the X scale is q_n^{-1}, which is simply one cell of the resonance chain (see Fig.4).

In the standard-map approximation we have

$$y_c(t) \;\approx\; \dot{x}_c(t) \;=\; 2\pi r_c + \sum_q b_q \cos(q\xi_c - 2\pi p t)$$

with $b_n = 2\pi a_n \nu_n$, and the transverse scaled amplitude is

$$B = b_n q_n^2 \sim 1 \tag{3.16}$$

Hence, the y scale is q_n^{-2}, the resonance width.

Consider now the periodic orbit at the resonance center (Fig.4). Its stability is determined by the Greene residue [33] (see also ref. [5])

$$R = \sin^2(\frac{t_n \omega_n}{2}) \sim 1 \tag{3.17}$$

where $t_n = q_n$ is the period, and $\omega_n \approx q_n v_n^{1/2}$ is the small oscillation frequency (see eq. (3.12)). Obviously, R is the scaled variable.

Finally, the scaled rotation number, or rather the scaled detuning

$$D = \rho_n q_n^2 \sim 1 \tag{3.18}$$

determines actually all the other scaled variables.

So far we considered exactly critical conditions that is $K = K_c(r)$. What would be the impact of any deviation $\Delta K = K - K_c(r) \neq 0$? It can be evaluated as follows. The perturbation amplitudes v_n in eq. (3.12) appear in q_n-th order of the perturbation theory and are proportional to $(K/K_c)^q = \exp(q \ln \frac{K}{K_c})$. Hence, for a small deviation from criticality ($\Delta K \to 0$) the amplitude $v_n \sim \exp(C q_n \Delta K)$ with some $C \sim 1$. At $\Delta K = 0$ the exponential dependence cancels, and only a power law (3.14) remains. Generally,

$$v_n \sim \frac{1}{q_n^4} \exp\,(C q_n \Delta K) \tag{3.19}$$

For $\Delta K > 0$ all scales $q_n \geq (\Delta K)^{-1}$ are destroyed and a chaotic layer of width $\Delta y \sim (\Delta K)^2$ is formed.

From eq. (3.19) the scaled perturbation can be introduced

$$P = q_n \Delta K_n \sim 1 \tag{3.20}$$

which describes the approach to the renormalization limit for a fixed v, for example.

If the original perturbation is non-analytic, i.e., has a power law spectrum $v_q^0 \sim q^{-\beta-1}$ (cf. model (1.3) where $f_m \sim m v_m^0$), the critical conditions are only possible

for $\beta > 3$, otherwise $K_c = 0$. Thus, $\beta_c = 3$ is the critical smoothness of the perturbation. I shall come back to this point in section 4.1 below.

3. The renormalization group [21]. This powerful method, well known and widely applied in hydrodynamical turbulence, phase transitions and quantum field theory, was first used in nonlinear dynamics and chaos theory in ref. [33]. Later on, the exact renormalization equations were formulated and studied in ref. [34] for (dissipative) 1D maps, and in ref. [21] for 2D area-preserving (Hamiltonian) maps. The renormalization group equations are an abstract map acting in the space of dynamical maps, and it is based on the arithmetical map for successive convergents $r_n = p_n/q_n$ of the critical rotation number $r_c = (m_n)$:

$$\overline{p} = \overline{m}p + \underline{p} \ ; \ \overline{q} = \overline{m}q + \underline{q} \tag{3.21}$$

where $\overline{p} \equiv p_{n+1}$; $p \equiv p_n$; $\underline{p} \equiv p_{n-1}$ etc. Besides qualitative understanding of critical phenomena (particularly, their universality) this approach provides very efficient numerical algorithms for computing all the parameters of the critical structure. In contrast, our resonant theory, being inherently approximate, allows some analytical estimates.

The resonance overlap criterion, on which the theory is essentially based, can directly provide order-of-magnitude estimates only, for example, for scaled variables (3.14-3.17). However, there exists another group of critical parameters which can be evaluated to a surprising accuracy. Those are the scaling factors, that is the ratios of particular quantities on the neighbouring scales. For example,

$$s_a = \frac{a_n}{a_{n+1}} \ ; \ s_b = \frac{b_n}{b_{n+1}} \ ; \ s_K = \frac{\Delta K_n}{\Delta K_{n+1}}$$

are the renormalization factors for x, y , and the perturbation K , respectively.

The structure of scaled variables shows that all scaling factors are some powers of the main arithmetical factor

$$s_q = \frac{q_n}{q_{n-1}} \tag{3.22}$$

To compare both approaches let us consider the simplest case of a homogeneous continued fraction $r = [m, m, ..., m, ...] \equiv [m^\infty]$. In this case all the scaled variables become asymptotically, as $n \to \infty$, exact invariants of the renormalization group. This is called the scale invariance. For example, $D \to (4 + m^2)^{-1/2}$ (see eq. (3.21)) which is a simple arithmetical property. The other invariants are not yet known except the case of $r = r_G = (1^\infty) = (\sqrt{5} - 1)/2 = 0.618...$ which is called the golden tail (because for asymptotic properties only the tail of the continued fraction matters).

In this particular case, studied in great detail, the renormalization invariants are: $T = 1$ (if, by definition, $t_n = q_n$, see eq. (3.13)); $R = 0.2500888...$; $V \approx (2 \arcsin \sqrt{R})^2 = 1.097052...$; $A \approx 0.167$; $B \approx 2\pi A/\sqrt{5} \approx 0.470$. Notice that from the above relation $R \sim V \sim \Delta\rho_n/\rho_n$ the Greene residue also characterizes the resonance overlap.

Now consider the scaling factor for the area $c_n \sim a_n b_n$ of a resonance cell (the corresponding scaled variable $C = c_n q_n^3 \approx AB \approx 0.0787$):

$$s_c = c_n/c_{n+1} = s_q^3 = 4.236... \tag{3.23}$$

while the exact numerical value via the renormalization group is 4.339... The two numbers are not equal but very close which was a puzzle for the formal renormalization group approach.

A similar situation arises for the perturbation factor: $s_K = s_q = 1.618...$ (resonant theory), and $s_K = 1.627...$ (numerically).

The differences in scaling factors of the two theories can be interpreted as small changes of the exponents of q in scaled variables. For the two examples above we can write:

$$\begin{aligned} C &= c_n q_n^{\alpha} \ ; \ \alpha = 3.049960... \\ P &= \Delta K_n q_n^{\beta} \ ; \ \beta = 1.0126966... \end{aligned} \tag{3.24}$$

Other examples will be given below.

The behavior of the asymptotic renormalization invariants A and R is shown in Fig.6 below. Remarkably, the invariant critical structure, which repeats itself on finer

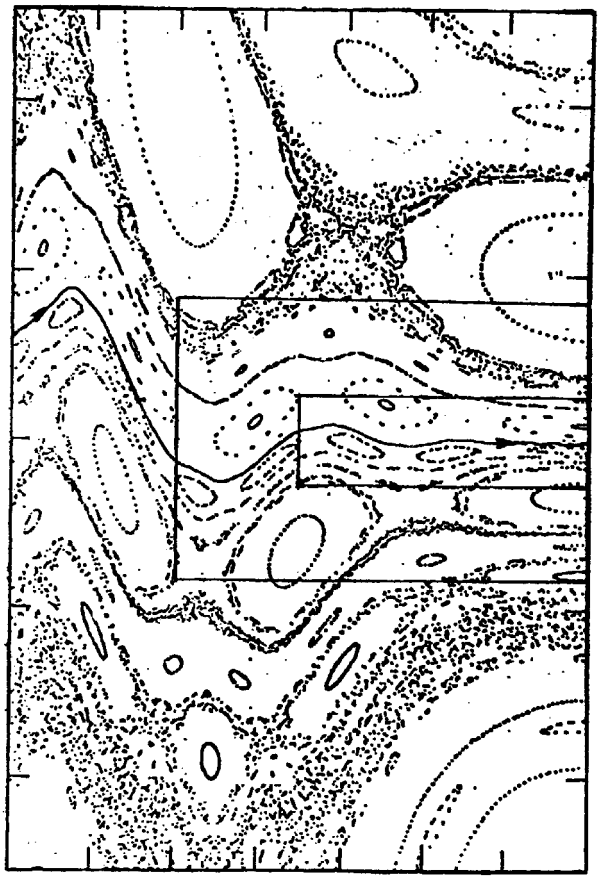

Figure 5. A small part of the critical structure with 3 successive scales shown by rectangles (including the whole picture). The critical curve is indicated by 2 arrows (after ref. [21]).

and finer scales with rapidly increasing precision, is itself of the highest complexity as it contains both chaotic trajectories and an intricate admixture of regular and chaotic components of motion. An example of a tiny part ($\sim 0.01 \times 0.01$) of that structure is shown in Fig.5 [21]. The scale invariance is clearly seen within 3 successively scaled areas indicated by rectangles.

Notice that the scale invariance holds on a particular discrete but infinite set of scales, because the renormalization group equations are based on the arithmetical map (3.21).

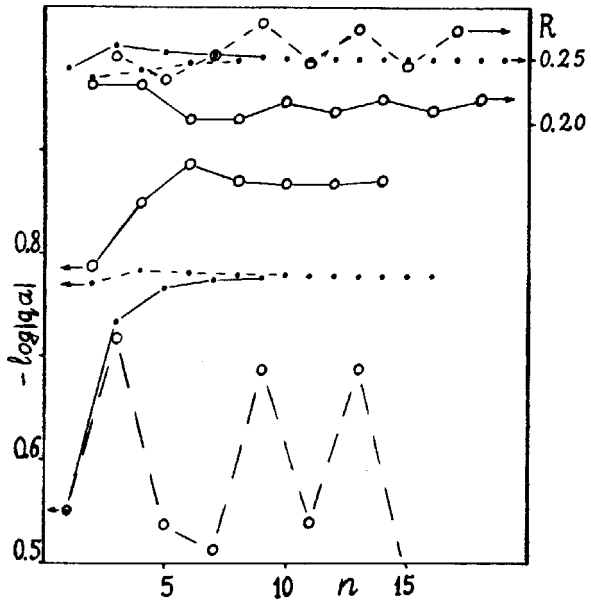

Figure 6. An example of renormalization chaos for a random r_c (circles). Arrows indicate the corresponding scales for $A = a\,q$ (lower part) and for R (upper part); n is the renormalization time (the number of a principal scale). For comparison the same data are given for $r = r_c$ (dots) which illustrate the scale invariance (after ref. [30]).

4. Renormalization chaos [22]. Variation of the critical structure from scale to scale can be viewed as some abstract dynamics. The corresponding dynamical space is infinite dimensional but we may consider various few-dimensional projections of that as described by a set of scaled variables such as A_n, R_n, V_n etc. (see, e.g., Fig.6). The serial scale number n plays a role of 'time', and we call it the renormalization time. It is proportional to the logarithm of spatial and temporal scales:

$$n \sim |\ln a_n| \sim |\ln b_n| \sim \ln t_n \sim \ln q_n \tag{3.25}$$

The renormalization time is discrete as is the renormalization dynamics based on the arithmetical map (3.21).

The scale invariance described in the previous section is the simplest type of renormalization dynamics, namely, a fixed point of the renormalization map. The dynamical interpretation of renormalization suggests other, more complicated, scalings up to a chaotic one which would be the opposite limiting case. Guided by this heuristic ap-

proach we conjectured a new type a chaotic behavior - the renormalization chaos [22], and presented an example of the latter in ref.[30]. A similar possibility was also considered in ref. [35] for dissipative systems as modelled by an 1D map.

Our basic idea was to achieve the most complicated renormalization by using a random critical rotation number, a rotation number with a random sequence of the continued fraction entries m_n . As is known from the modern ergodic theory (see, e.g., ref. [20]) this is the case for almost any irrational r . Indeed, we may introduce a sequence of rotation numbers via the Gauss map

$$r = \frac{1}{m + \overline{r}} \;\; ; \;\; \overline{r} = \frac{1}{r} \; mod \; 1 \tag{3.26}$$

which is known to be chaotic [20]. Moreover, the basic arithmetical factor in the renormalization (3.22) also obeys the same map

$$\omega = \frac{1}{\overline{\omega}} \; mod \; 1 \;\; ; \;\; \omega = \frac{1}{s_q} < 1 \tag{3.27}$$

backwards in renormalization time, and with the 'initial' $\omega_\infty = \tilde{r}$ where $\tilde{r}$ is the irrational with reversed sequence of elements in respect to r . Clearly, the variation of critical structure in this case would be as random and unpredictable as a chaotic trajectory. An example of renormalization chaos is presented in Fig. 6 as described by A and R scaled variables. The irregular character of this renormalization dynamics is clear from Fig. 6, and the proof of its randomness is related to the Gauss map (3.27).

A chaotic trajectory is completely determined, in principle, by the initial conditions via the formal equations of motion. By analogy, we can conjecture that the chaotic variation of critical structure is related to the rotation number r . This would imply that the scaled variables are some universal functions of r . Then, asymptotically, as $n \to \infty$, the renormalization dynamics is described by an infinite dimensional map

$$\overline{A}(r) = A(\overline{r}) \;\; ; \;\; \overline{R}(r) = R(\overline{r}) \;\; etc. \;\; ; \;\; \overline{r} = \frac{1}{r} \; mod \; 1 \tag{3.28}$$

Some numerical confirmation of this conjecture was presented in ref. [30]

Thus, particular critical structure essentially depends on r , and in this sense is not universal. Nevertheless, the statistical properties of chaotic renormalization are the same for almost any r . Particularly, the average arithmetical factor (3.22)

$$< s_q > = \; e^{h/2} \approx 3.28 \;\; ; \;\; h = \frac{\pi^2}{6 \ln 2} \approx 2.37 \tag{3.29}$$

where h is the KS-entropy of the Gauss map (3.27). This may be compared with a non-generic case of the scale invariance for $r = [m^\infty]$:

$$s_q = \frac{m + \sqrt{4 + m^2}}{2} \to 1.618... \tag{3.30}$$

Numerical value is given for $m = 1$ (golden tail).

A grand example of renormalization chaos is the oscillation of the whole universe near the singularity in the homogeneous but anisotropic cosmological models [36]. So far there is no sign of such oscillations in our early Universe. Yet, the equations of the general relativity allow that type of solution. Remarkably, the very complicated relativistic equations are here approximately reduced to the trivial Gauss map.

5. Higher dimensions

A general picture of overlapping resonances, which destroy KAM tori, holds for arbitrary number of degrees of freedom [7]. This allows us to extend our resonant theory of critical phenomena to higher dimensions. There are two generally different cases of the latter: (i) $N > 2$ degrees of freedom, and (ii) a driving quasiperiodic perturbation of one degree of freedom. In the resonant theory both are similar, the principal parameter being the number of frequencies N [37].

First of all, for arbitrary N the number of all resonances with $\sim q$ harmonics of each basic frequency is $\sim q^N$, hence the detuning $\rho \sim q^{-N}$ (cf. eq. (3.9)), and

$$D = \rho q^N \sim 1 \tag{3.31}$$

Now the main rotation number r is defined with respect to one of the perturbation frequencies. The remaining $N-2$ rotation numbers enter as driving frequencies $\nu_q \sim q\rho \sim q^{1-N}$ in the critical Hamiltonian (3.12). The resonance width $\Delta\rho \sim v_q^{1/2}$, and from the overlap criterion (3.10) the criticality condition is $v_q \sim q^{-2N}$, or (cf. eq. (3.14))

$$R \sim V = v_q q^{2N} \sim 1 \tag{3.32}$$

Hence, the critical perturbation smoothness $\beta_c = 2N - 1$ increases with N (cf. ref. [37]).

Longitudinal amplitudes $a_q \sim qv_q/\nu_q^2 \sim q^{-1}$ of the critical motion $x_c(t)$ do not depend on N, and

$$A = qa_q \sim 1 \tag{3.33}$$

as before. The transverse amplitudes $b_q \sim a_q\nu_q \sim q^{-N} \sim \Delta\rho$ decrease with N but remain of the order of the width of the resonances. Finally, the perturbation scaling does not, approximately, depend on N:

$$P = q\,\Delta\,K_q \sim 1 \tag{3.34}$$

However, in the many-dimensional case ($N > 2$) there is no simple procedure to single out the principal resonances like for $N = 2$.

The renormalization group in higher dimensions was generally discussed already for dissipative systems (see, e.g., ref. [35]). Yet, I am not aware of any particular results concerning the scaling properties in such systems.

To the best of my knowledge the only numerical data for $N = 3$ (standard map with a time-periodic parameter $K(t)$) were presented recently in ref. [23]. They seem to confirm the scalings related to R, P and A.

On the other hand, the authors did not find the scale invariance in this model, and it seems that it does not exist at all. What is even more important, they discovered a breakdown of the renormalization universality in the sense that irregular oscillations of the critical structure depend, generally, not only on the two rotation numbers but also on the parameters of the model. Thus, many-dimensional renormalization dynamics appears to be even more complicated (chaotic?) as compared to the simplest case $N = 2$.

4 Critical Statistics

The most difficult, and as yet unsolved, problem is the impact of the critical structure at the chaos border on the statistical properties of motion.

1. Smooth perturbation: $\beta < \beta_c$. To begin with, let us consider a simpler problem of a smooth perturbation (1.3) with $\beta < \beta_c = 3$. First, we can calculate β_c directly from the resonance overlap criterion as applied to the original perturbation (1.3). The simplest estimate is as follows. The total width of all primary resonances $r_{pq} = p/q$ on the unit r interval is

$$\sim \sum_q q v_q^{1/2} \sim K^{1/2} \sum_q q^{\frac{1-\beta}{2}} \sim 1 \tag{4.1}$$

This sum diverges for $\beta \leq 3$, hence $\beta_c = 3$ in agreement with the previous estimate in section 3.2. The latter estimate in eq. (4.1) determines those resonances which provide the overlapping for $\beta < 3$. The critical $q_c \sim K^{(\beta-3)^{-1}}$. The corresponding resonance width $\Delta\rho_c \sim K^{1/2} q_c^{-(\beta+1)/2}$, and the frequency (cf. eq. (3.17)) $\omega_c \sim q_c \Delta \rho_c$. Hence, the diffusion rate in r (or in y) is

$$D \sim \omega_c (\Delta\rho_c)^2 \sim K^{3/2} q_c^{-\frac{1+3\beta}{2}} \sim K^{\frac{5}{3-\beta}} \tag{4.2}$$

The border case $\beta = 3$ requires more accurate estimates.

Estimate (4.2) agrees with numerical results in ref. [38] for $\beta = 1$ (discontinuous $f(x)$).

2. Critical perturbation [31]. One peculiarity of the standard map (1.6) is the periodicity not only in x but also in y with the same period 2π . As a result there is exact critical perturbation $K = K_G \approx 1$ [33], such that for $K > K_G$ the motion is unbounded in y and diffusive for some initial conditions (section 2.3). The problem I am going to discuss now is to explain the scaling (2.3) for the diffusion rate as $K \to K_G$.

For $K > K_G$ the last (most robust) KAM curve is destroyed and transformed into a chaotic layer comprising all critical scales $q_n \geq q_\epsilon$ where $q_\epsilon \sim \epsilon^{-1}$, and $\epsilon = K - K_G \to 0$ (see eq. (3.19) and around). This chaotic layer is just the critical 'bottleneck' which controls the transition time between integer resonances $r = m$, and, hence, the global diffusion. The time scale in the layer is $\sim q_\epsilon$, and so is the exit time (t) from the layer. However, penetration into this thin layer ($\Delta r_\epsilon \sim q_\epsilon^{-2}$, eq. (3.16)) from a big region ($\Delta r \sim 1$) takes much longer time:

$$t_+ \sim t_- \frac{\Delta r}{\Delta r_\epsilon} \sim q_\epsilon^3 \sim \epsilon^{-3} \sim D^{-1} \tag{4.3}$$

This determines the transition time inversely proportional to the diffusion rate D, in agreement with recent numerical results (see eq. (2.3) and ref. [18]). Notice that the first value for the exponent ≈ 2.6 [7] was not very accurate. The above estimate $\Delta r_\epsilon / t_- \sim \Delta r / t_+$ (4.3) is simply the flow balance in statistical equilibrium.

It is interesting to note that the renormalization group theory [39] gives the value $\ln s_c / \ln s_K = 3.011...$ This is another example of the surprising accuracy of the apparently primitive resonant theory.

3. The chaos border [30]. The impact of the critical structure at the chaos border in phase space on the statistical properties of the chaotic motion is the most difficult, and as yet unsolved, problem. The straightforward approach would be as follows. The transition time τ_n between adjacent scales is proportional to the time scale $t_n \sim q_n$

which, in turn, scales like $\mu_n^{-1/2} \sim C_y^{-1/2}$ where $\mu_n \sim \rho_n \sim q_n^{-2}$ is the sticking measure, and where C_y is the correlation (section 3.1 and 3.2). Hence, $C_y \sim \tau^{-2}$, and $p_c = 2$; $p = 3$. In a more sophisticated way the same result was obtained in ref. [40]. Unfortunately, this is in sheer contradiction with numerical data: $p \approx 1.5 < 2$.

The only way of avoiding this contradiction that I see is to conjecture that at the exact criticality all transition times $\tau_n = \infty$, i.e., that all scales are dynamically disconnected. Why does then a connected chaotic component near the chaos border exists? The natural answer is in that the exact criticality is achieved on the border only, while inside a chaotic region the motion is supercritical. Consider, for example, model (3.1). Locally it is described by the standard map with $K \approx \lambda/y$. In a small vicinity of the border $y = y_b \approx \lambda$, the perturbation K indeed increases like $\Delta K \sim \Delta y \sim \rho \sim q^{-2}$. However, this is not enough to destroy the corresponding scale q_n, as $q_n \Delta K_n \sim q_n^{-1} \ll 1$ (see eq. (3.19)). Only resonances with $q \geq Q_n \sim q_n^2$ would be destroyed and they form a very narrow ($\sim Q_n^{-2} \sim q_n^{-4}$) chaotic layer which could play a role of the bottleneck controlling the transition time τ_n . Similarly to derivation of eq. (4.3) we obtain

$$\tau_n \sim Q_n \frac{Q_n^2}{q_n^2} \sim q_n^4 \sim \mu_n^{-2} \sim C_y^{-2} \tag{4.4}$$

Hence

$$C_y(\tau) \sim \tau^{-1/2} \; ; \; P(\tau) \sim \tau^{-3/2} \tag{4.5}$$

now in agreement with numerical data.

The same result can be obtained in a different, more formal, way. Namely, we can rescale the dependence (4.3) for the transition between integer resonances ($q_n = 1$) to arbitrary scale q_n . To this end we rewrite eq. (4.3) in scaled variables

$$\frac{\tau_n}{t_n} \sim (q_n \Delta K)^{-3} \tag{4.6}$$

With $t_n \sim q_n$ and $\Delta K \sim q_n^{-2}$ we arrive at eq. (4.4). Notice that a different relation $\tau_n(q_n)$ in ref. [22] was due to a mistake in scaling.

A weak point of the latter approach (4.6) is that the scaling (4.3) is asymptotic ($q_n \to \infty$), while the integer resonances ($q_n = 1$) are not. In any event, further studies into the mechanism of critical statistics are certainly required.

In higher dimensions (section 3.5) the supercriticality $\Delta K \sim \rho \sim q^{-N}$; the bottleneck harmonic is $Q \sim (\Delta K)^{-1} \sim q^N$, and the transition time (cf. eq. (4.4)) is given by

$$\tau \sim Q^{N-1} \frac{Q^N}{q^N} \sim Q^{2N-2} \sim \mu^{2-2N} \tag{4.7}$$

Hence

$$C_y \sim \mu \sim \tau^{-\frac{1}{2N-2}} \; ; \; p_c = \frac{1}{2N-2} \tag{4.8}$$

As $N \to \infty$, $p_c \to 0$, and correlations do not decay at all. I am going to come back to this interesting case in section 4.5 below.

Another difficult problem is the arithmetic of rotation numbers r_b of the critical border curves. In ref. [22] it was conjectured that the set of r_b consists of all combinations of only two elements $m = 1$ and 2 in the continued fraction representation. This is sufficient for r_b to be random, and hence to explain the irregular oscillation of the local exponent in the distribution of Poincaré recurrences (section 3.1). This conjecture was partially confirmed numerically in ref. [45]. Our recent refined conjecture is that r_b are the so-called Markov numbers [30].

4. Internal borders. Typically, the central part of principal critical resonances is not destroyed (see, e.g., Fig.5). Hence, in any neighborhood of the main chaos border there is an infinite set of internal chaos borders, each one with its own critical structure. Assuming universality of critical phenomena at any chaos border we arrive at the following estimate in scaled variables

$$(\mu_c q^2) \sim (\frac{\tau}{q})^{-p_c} \tag{4.9}$$

for a principal resonance q where μ_q is the sticking measure at the internal border.

The main difficulty here is that the internal borders exists not only inside the principal resonances but also in many others, near the critical border curve, which are not destroyed by the local supercritical perturbation. To estimate the total number of such resonances we can make use of eq. (3.19) which determines the stability zone $\Delta K_s \sim \rho_s \sim q^{-1}$ for any q (as a very crude approximation, of course). Then, for a given q only $M_q/q \sim 1$ resonances fall into this zone, where $M_q \sim q$ is the total number of resonances p/q for a fixed q. Again, as a crude approximation we can extend the estimates, particularly eq. (4.19), on all undestroyed resonances. As a result, the total internal border contribution to the correlation is

$$\tilde{C}_y \sim \sum_q \mu_q \sim \tau^{-p_c} \sum_q^{\tau} q^{p_c-2} \tag{4.10}$$

where the sum is taken over all q up to τ. This contribution is essential if $p_c \geq 1$. But for $p_c > 1$ the above estimate is not self-consistent as $\tilde{C}_y \sim \tau^{-1}$, contrary to assumed universality. However, the latter holds for $p_c = 1$, to logarithmic accuracy. This was the preliminary conclusion in ref. [41] which was also confirmed in ref. [42].

This would be a nice solution in the spirit of universality of the critical phenomena. Yet, first, the value $p_c = 1$ seems still to be incompatible with numerical data (section 3.1), and second, there is another possibility missed in ref. [41], namely, $p_c < 1$, as is suggested by numerical data. Then, the effect of internal borders is not decisive, at least, for the exponent p_c whose value is determined by another mechanism, for example, the one described in the previous section.

In higher dimensions we have instead of eq. (4.9) (see section 3.5)

$$(\mu_q q^N) \sim (\frac{\tau}{q^{N-1}})^{-p_c} \tag{4.11}$$

In calculating the total contribution of all internal borders we need to take into account that now there are as many as $\sim q^{N-2}$ undestroyed resonances, for a given q, within the stability zone. Hence, the total 'internal' correlation is

$$\tilde{C}_y \sim \sum_q \mu_q q^{N-2} \sim \tau^{-p_c} \sum_q^{\tau^{1/(N-1)}} q^{p_c(N-1)-2} \tag{4.12}$$

The critical value p_c^* of the critical exponent is $p_c^* = (N-1)^{-1}$. Only this value preserves universality based entirely on the internal borders. And, again, there is another possibility that $p_c < p_c^*$ so that internal borders are irrelevant. This is just the case if the above estimate (4.8) is true: $p_c = p_c^*/2$.

Preliminary numerical results obtained in collaboration with V.V. Vecheslavov ($p_c \approx 0.26$ and 0.19 for N=3 and 4, respectively) seem to confirm (or, at least, do not contradict) prediction (4.8).

5. Superfast diffusion [22]. Slow correlation decay with $p_c < 1$ (4.5) may result in a superfast diffusion. Indeed, if this correlation determines the diffusion, the rate

$$D_Z \sim \int C_y(\tau) d\tau$$

formally diverges. Here the diffusion proceeds along a new variable Z, and $\dot{Z} = Y$. The divergence means that the dispersion (the second moment of the distribution function)

$$\sigma^2 \sim \int D d\tau \sim t^{2-p_c} \tag{4.13}$$

grows faster than the time t, hence we describe this as the 'superfast diffusion'. This phenomenon was studied from different points of view in many papers (see, e.g., refs. [43,44]).

The simplest example is again the standard map for special values of the parameter $K \approx 2\pi m$, with any integer $m \neq 0$. At these K the so-called accelerator modes exist [7], i.e., relatively small areas of regular motion with linearly increasing momentum: $y \sim \pm t$, while the phase x is fixed. A chaotic trajectory cannot penetrate into these domains but it does stick to their borders. As a result, a superfast diffusion in y occurs, which was first observed numerically in ref. [46]. Notice that in the above notation $z = y$, while the role of y is now played by a new coordinate normal to the chaos border surrounding the regular regions. According to eq. (4.13)

$$\sigma^2 \approx \alpha \mu_s \frac{K^2}{2} t^{3/2} \sim t^{3/2} \tag{4.14}$$

where $\alpha \approx 0.5$ from numerical data [46] for $K \approx 2\pi$, and relative stable area $\mu_s \approx 0.02$. As $\mu_s \sim K^{-2}$ [7], the rate of this anomalous diffusion ($\sigma^2/t^{3/2}$) does not depend either on $K \to \infty$ or on $\mu_s \to 0$.

In ref. [44,47] more complicated accelerator modes were shown to produce a superfast diffusion, corresponding to $p_c \approx 2/3$, in reasonable agreement with our numerical data. A simple expression for the growth of all moments of the distribution function was also given in ref. [44], namely:

$$\sigma^k \sim t^{k-p_c} \tag{4.15}$$

for k even. In higher dimensions when $N \to \infty$ and $p_c \to 0$ this relation becomes especially simple but somewhat puzzling. It appears to describe an almost free motion, but in both directions of the Z variable! The limiting case $p_c = 0$ corresponds to the fastest homogeneous diffusion possible.

Further insight into the nature of superfast diffusion can be obtained from the dynamical power spectrum, i.e., the Fourier transform of the correlation [30]. For $\omega \to 0$ we have from eq. (4.8)

$$S_y(\omega) \sim \omega^{p_c-1} \sim \omega^{-\frac{2N-3}{2N-2}} \tag{4.16}$$

As $N \to \infty$, it approaches the famous $1/\omega$ spectrum which, thus, produces the fastest diffusion. If $\dot{Z} = y$, the spectrum of the Z-motion is

$$S_Z = \frac{S_y}{\omega^2} \sim \omega^{p_c-3} \tag{4.17}$$

From normalization (Parseval's theorem)

$$\overline{Z^2} = \int S_Z(\omega)d\omega \sim \omega^{p_c-2} \sim t^{2-p_c} \tag{4.18}$$

If $p_c < 1$ the integral diverges as $\omega \to 0$. For a finite time interval the minimal $\omega \sim t^{-1}$, and the diffusion law (4.13) is recovered, including the limiting $p_c = 0$. However, in the latter case the velocity dispersion $\overline{y^2} \sim \ln\omega$ diverges (see eq. (4.16)). In our models with a chaos border this is impossible, so $p_c > 0$ always.

The theory of superfast diffusion can be applied to a broad variety of different problems. A nice example is the tangle of a long polymeric molecule in a certain environment. Such molecule can be considered approximately as a trajectory of the self-avoiding random walk. The constraint imposes a long-term correlation which can be estimated as follows. Suppose that the molecule length l and the tangle size σ are related by

$$\sigma^2 \sim l^{2\nu} \tag{4.19}$$

with some so far unknown parameter ν. The correlation due to avoided crossings of the molecule line is then roughly proportional to the probability of the self-crossing:

$$C \sim \frac{l}{\sigma^d} \sim l^{1-\nu d} \tag{4.20}$$

where the integer d is the space dimension. Hence, we have a power-law correlation with the exponent $p_c = \nu d - 1$. Using eq. (4.13) with $t = l$ and eq. (4.19) we arrive at the relation

$$2\nu = 3 - \nu d \;\; ; \;\; \nu = \frac{3}{2+d} \tag{4.21}$$

which is known as Flory's formula (see, e.g., ref. [48]). It was derived in a completely different way (from the thermodynamics of a polymeric molecule), and holds for $d \leq 4$, otherwise $\nu = 1/2$. In our dynamical approach the latter limitation follows from the condition $p_c < 1$ for anomalous diffusion. In the border case $\sigma^2 \sim l \ln l$ (see, e.g., T. Geisel et al. in ref. [43]), which slightly differs from Flory's formula.

6. Fractal properties [49]. The critical structure in Hamiltonian systems is also called 'random fractals' (R.Voss, ref. [43]) because of the renormalization chaos (section 3.4), or 'fat fractals' [49] for carrying a finite measure in contrast to dissipative systems. Some fractal properties were studied numerically in ref. [49].

Here I am going to explain one property - the fractal dimension d_L of the set of all chaos borders (mainly internal ones, of course). It is inferred from the dependence of the measure μ_{ch} of a chaotic component on the spatial linear resolution $\epsilon \to 0$:

$$\mu_{ch}(\epsilon) = \mu_{ch}(0) + \alpha\,\epsilon^{\beta} \tag{4.22}$$

Here $\mu_{ch}(0) > 0$ is the measure of the whole chaotic component. Hence, its topological dimension is $d_s = 2$. The second term represents the borders whose total length and dimension are

$$L(\epsilon) \sim \epsilon^{\beta-1} \;\; ; \;\; d_L = 2 - \beta \tag{4.23}$$

The simplest evaluation of this scaling can be done as follows (see section 4.4). Each surviving resonance has internal borders of total length $l_q \sim 1$. This estimate follows

from the fact that an individual border is a curve of topological dimension $d_l = 1$. This is so because the ratio of transverse to longitudinal scaling factors of the critical structure $s_b/s_a = q_n \to \infty$ as $n \to \infty$ (see sections 3.2 and 3.3). Thus, the border curve $y_b(x)$ is very smooth (see Fig.5). The number of surviving resonances is of the order of maximal $q = q_{max}$, determined by the resolution $\epsilon \sim q_{max}^{-2}$. Hence

$$L \sim \epsilon^{-1/2} \; ; \; \beta = \frac{1}{2} \; ; \; d_L = \frac{3}{2} \tag{4.24}$$

in reasonable agreement with the numerical result $\beta = 0.4 - 0.7$ [49].

Notice, also, that the total number of resolved borders scales, in this approximation, as

$$N_b \sim q_{max}^2 \sim \epsilon^{-1} \tag{4.25}$$

In higher dimensions with N frequencies we need to consider an N-dimensional map with non-fractal border surfaces of $N-1$ dimensions. Now there are $\sim q^{N-1}$ surviving resonances up to $q_{max} \sim \epsilon^{-1/N}$. The border surface in each such resonance $S_1 \sim 1$, and the total border surface and its dimension are

$$S_b \sim \epsilon^{-(1-\frac{1}{N})} \; ; \; d_S = N - \frac{1}{N} \tag{4.26}$$

The total number of resolved border surfaces, or of the domains with regular motion

$$N_b \sim \epsilon^{-1} \tag{4.27}$$

does not depend on N, and in this sense it is universal.

Acknowledgements

I would like to express my sincere gratitude to D.L.Shepelyansky, my main collaborator in the studies of critical phenomena, to F.Vivaldi who attracted our attention to this interesting problem, and to G.Casati, D.Escande, R.MacKay, I.Percival and Ya.Sinai for stimulating discussions.

References

[1] V.M. Alekseev and M.V. Yakobson, Phys. Reports **75** (1981) 287.

[2] G. Chaitin, Information, Randomness and Incompleteness (World Scientific, 1990).

[3] B.V. Chirikov, F.M. Izrailev and D.L. Shepelyansky, Physica D **33** (1988) 77.

[4] B.V. Chirikov, Time-Dependent Quantum Systems, Proc. Les Houches Summer School on Chaos and Quantum Physics (Elsevier, 1990).

[5] A. Lichtenberg, M. Lieberman, Regular and Stochastic Motion (Springer, 1983).

[6] G.M. Zaslavsky, Chaos in Dynamic Systems (Harwood, 1985).

[7] B.V. Chirikov, Phys. Reports **52** (1979) 263.

[8] B.V. Chirikov and V.V. Vecheslavov, Astron. Astroph. **221** (1989) 146.

[9] G. Casati et al., Phys. rev. A **36** (1987) 3501.

[10] A.A. Chernikov, R.Z. Sagdeev and G.M. Zaslavsky, Physica D **33** (1988) 65.

[11] B.V. Chirikov, Foundations of Physics **16** (1986) 39.

[12] M. Eisenman et al., Lecture Notes in Physics **38** (1975) 112; J.von Hemmen, ibid., **93** (1979) 232.

[13] B.G. Konopelchenko, Nonlinear Integrable Equations, Lecture Notes in Physics **270** (1987).

[14] B.V. Chirikov and V.V. Vecheslavov, KAM integrability, in: Analysis etc. (Academic Press, 1990) p.219.

[15] V.I. Arnold and A. Avez, Ergodic Problems in Classical Mechanics (Benjamin, 1968).

[16] B.V. Chirikov, Proc. Roy. Soc. Lond. A **413** (1987) 145.

[17] A. Rechester et al. Phys. Rev. A **23** (1981) 2664.

[18] B.V. Chirikov, D.L. Shepelyansky, Radiofizika **29** (1986) 1041.

[19] F. Vivaldi, private communication.

[20] I. Kornfeld, S. Fromin and Ya. Sinai, Ergodic Theory (Springer, 1982).

[21] R. MacKay, Physica d **7** (1983) 283.

[22] B.V. Chirikov and D.L. Shepelyansky, Physica D **13** (1984) 395.

[23] R. Artuso, G. Casati and D.L. Shepelyansky, 1990 (to appear).

[24] B.V. Chirikov, D.L. Shepelyansky, Proc. 9th Int. Conf. on Nonlinear Oscillations, Kiev, 1981, Vol.2, p.421. (Kiev, Naukova Dumka, 1983) English translation available as preprint PPL-TRANS-133, Plasma Physics Lab., Princeton Univ., 1983.

[25] S. Channon and J. Lebowitz, Ann. N.Y. Acad. Sci **357** (1980) 108.

[26] G. Paladin and A. Vulpiani, Phys. Reports **156** (1987) 147.

[27] C. Karney. Physica D **8** (1983) 360.

[28] P. Grassberger and I. Procaccia, Physica D **13** (1984) 34.

[29] J. Bene, P. Szépfalusy and A. Fülöp, A generic dynamical phase transition in chaotic Hamiltonian systems, Phys. Rev. Lett. (to appear).

[30] B.V. Chirikov and D.L. Shepelyansky, Chaos Border and Statistical Anomalies, in: Renormalization Group, D.V. Shirkov, D.I. Kazakov and A.A. Vladimirov (eds.), p. 221. (World Scientific, Singapore, 1988).

[31] B.V. Chirikov, Intrinsic Stochasticity, Proc. Int. Conf. on Plasma Physics, Lausanne, 1984, Vol. II, p.761.

[32] G. Schmidt and J. Bialek, Physica D **5** (1982) 397.

[33] J. Greene, J.Math.Phys. **9** (1968) 760; **20** (1979) 1183.

[34] M. Feigenbaum, J.Stat.Phys. **19** (1978) 25; **21** (1979) 669.

[35] S. Ostlund et al.,Physica D **8** (1983) 303.

[36] E.M. Lifshits et al., Zh.Eksp.Teor.Fiz. **59** (1970) 322; ibid (Pisma) **38** (1983) 79; J. Barrow, Phys. Reports **85** (1982) 1.

[37] B.V. Chirikov, The Nature and Properties of the Dynamic Chaos, Proc. 2d Int.Seminar "Group Theory Methods in Physics" (Zveingorod, 1982), Vol.1, p.553. (Harwood, 1985).

[38] I. Dana et al., Phys.Rev.Lett. **62** (1989) 233.

[39] R. MacKay et al., Physica D **13** (1984) 55.

[40] J. Hanson et al. J.Stat.Phys. **39** (1985) 327.

[41] B.V. Chirikov, Lecture Notes in Physics **179** (1983) 29.

[42] J. Meiss and E. Ott, Phys.Rev.Lett. **55** (1985) 2741; Physica D **20** (1986) 387.

[43] P. Lévy, Théorie de l'addition des variables eléatoires. (Gauthier-Villiers, Paris, 1937); T. Geisel et al. Phys.Rev.Lett. **54** (1985) 616; R. Pasmanter, Fluid Dynamic Research **3** (1988) 320; R. Voss, Physica D **38** (1989) 362; G.M. Zaslavsky et al., Zh.Exper.Teor.Fiz. **96** (1989) 1563.

[44] H. Mori et al., Prog.Theor.Phys. Suppl., 1989, No.99, p.1.

[45] J. Greene et al. Physica D **21** (1986) 267.

[46] C. Karney et al., ibid **4** (1982) 425.

[47] Y. Ichikawa et al., ibid **29** (1987) 247.

[48] P. de Gennes, Scaling Concepts in Polymer Physics. (Cornell Univ. Press., 1979).

[49] D. Umberger and D. Farmer, Phys.Rev.Lett. **55** (1985) 661; G. Grebogi et al., Phys.Lett. **A 110** (1985) 1.